

**Impact on ambient dose rate in metropolitan Tokyo
from the Fukushima Daiichi Nuclear Power Plant accident**

Kazumasa Inoue^{a,*}, Hiroshi Tsuruoka^a, Tan Van Le^a,
Moeko Arai^a, Kyoko Saito^b and Masahiro Fukushi^a

^a Department of Radiological Sciences, Graduate School of Human Health Sciences, Tokyo Metropolitan University, 7-2-10 Higashiogu, Arakawa-ku, Tokyo 116-8551, Japan

^b Department of Radiological Technology, Faculty of Health Sciences, Nihon Institute of Medical Science, 1276 Shimogawara, Moroyamamachi, Irumagun, Saitama 350-0435, Japan

* Corresponding author: Kazumasa Inoue, Ph.D.

7-2-10 Higashiogu, Arakawa-ku,

Tokyo 116-8551, Japan

Phone: +81-3-3819-1211

FAX: +81-3-6832-1406

Email: kzminoue@tmu.ac.jp

Highlights

- This car-borne survey provided the detailed dose distribution in metropolitan Tokyo.
- Ambient dose rate after the Fukushima accident was 24% higher than that before.
- Effective dose rate after the accident was 15% higher than the value for all of Japan.

Abstract

A car-borne survey was made in metropolitan Tokyo, Japan, in December 2014 to estimate external dose. This survey was conducted for all municipalities of Tokyo and the results were compared with measurements done in 2003. The ambient dose rate measured in the whole area of Tokyo in December 2014 was 60 nGy h^{-1} ($23 - 142 \text{ nGy h}^{-1}$), which was 24% higher than the rate in 2003. Higher dose rates ($> 70 \text{ nGy h}^{-1}$) were observed on the eastern and western ends of Tokyo; furthermore, the contribution ratio from artificial radionuclides (^{134}Cs and ^{137}Cs) to ambient dose rate in eastern Tokyo was twice as high as that of western Tokyo. Based on the measured ambient dose rate, the effective dose rate after the accident was estimated to be $0.45 \mu\text{Sv h}^{-1}$ in Tokyo. This value was 22% higher than the value before the accident as of December 2014.

Keywords

Ambient dose rate; Car-borne survey; Metropolitan Tokyo; Annual effective dose; Dose rate distribution map

1. Introduction

Large amounts of artificial radionuclides were released from the reactors into the environment in the March 2011 accident at the Fukushima Daiichi Nuclear Power Plant (F1-NPP) of the Tokyo Electric Power Company (TEPCO). The released amounts of artificial radionuclides, excluding those directly dispersed in the direction of the ocean, were estimated to be: $0.6-1.9 \times 10^{19}$ Bq of ^{133}Xe , $0.7-5.0 \times 10^{17}$ Bq of ^{131}I and $1.0-5.0 \times 10^{16}$ Bq of ^{137}Cs (Koo et al., 2014). For ^{137}Cs , this value is about 42% of the estimated amount emitted in the 1986 Chernobyl accident (Stohl et al., 2012). According to the simulation study by Koo et al. (2014), for the ^{137}Cs released into the atmosphere, 20% was deposited onto the land of Japan and the other 80% was transported to the ocean or other areas of the northern hemisphere. For the Japanese land deposition, most of the artificial radionuclides deposited on the ground in a northeastern area from the F1-NPP (Yoshikawa et al., 2014), but some of the artificial radionuclides were subsequently diffused within an altitude of 0-1000 m from ground level and deposited on southern and southwestern areas depending on the topography, wind direction and precipitation field (Kinoshita et al., 2011; Morino et al., 2011). Especially, the distribution of artificial radionuclides was affected by the land altitudes because the southern and southwestern areas from the F1-NPP are mixes of mountainous regions (altitudes of 600 – 800 m) and flatlands.

In metropolitan Tokyo (Fig. 1A), the artificial radionuclides were wet-deposited on March 21-23 by rainfalls (Kinoshita et al., 2011; Morino et al., 2011). In fact, artificial radionuclides such as ^{131}I , ^{132}I , ^{132}Te , ^{134}Cs , ^{136}Cs , and ^{137}Cs were observed on March 22 at the Canadian embassy located in Tokyo (Zhang et al., 2013). According to the results of air-borne monitoring done in September 2011 for Tokyo by the Ministry of Education, Culture, Sports, Science and Technology, Japan (Ministry of Education, Culture, Sports, Science and Technology, 2011), higher ambient dose rates were observed on the eastern and western ends of Tokyo. Air-borne radiation monitoring has been continuously performed, mainly by the Japan Atomic Energy Agency (JAEA) (Yuuki et al., 2014). The high dose rate areas (i.e. within 80 km from F1-NPP) continue to be conscientiously monitored; however, metropolitan Tokyo has not been included in those monitoring areas since May 2012. Andoh et al. (2015) have also made

car-borne surveys in eastern Japan since June 2011. However, the whole metropolitan Tokyo area has not been included in these surveys. The Tokyo Metropolitan Government also carried out measurement of the ambient dose rates at 1 m from the ground surface using NaI(Tl) scintillation survey meters at 100 locations in Tokyo in June 2011 (Tokyo Metropolitan Government, 2011). Currently, ambient dose rates at eight locations in Tokyo are provided on a website by the Tokyo Metropolitan Institute of Public Health (Tokyo Metropolitan Institute of Public Health, 2015). However, these “point” data are not sufficient to obtain a complete view of the ambient dose rate in Tokyo and to evaluate safeguarding of the health of area residents.

Measurements for the whole metropolitan Tokyo area should be continually performed to estimate the migration of radionuclides because ambient dose rate has been drastically changed by rainfall, natural decay of radionuclides and decontamination work. Especially, there have been no reports about the migration of artificial radionuclides in big cities which have large areas covered with asphalt and concrete. In addition, it is necessary to consider the presence of natural radionuclides such as ^{40}K , ^{238}U series and ^{232}Th series (i.e., background) to more accurately assess the impact from the accident. The authors recently reported detailed data for ambient dose rates ($n = 669$) measured in 2003 for Tokyo (excluding the Pacific Ocean islands that are within the Tokyo Government’s jurisdiction) (Inoue et al., 2015a). The arithmetic average ambient dose rates were 47 nGy h^{-1} ($18 - 61 \text{ nGy h}^{-1}$) in the eastern area of Tokyo (A1 in Fig. 1B) and 54 nGy h^{-1} ($34 - 76 \text{ nGy h}^{-1}$) in the western area (A2 in Fig. 1B), and there was some dependence of the dose rates on the geological age and the natural environments.

No severe nuclear power plant accident has occurred that engulfed a large metropolitan center such as Tokyo where 13.35 million people live (the F1-NPP is more than 200 km from Tokyo). Easy-to-understand and accurate information about ambient dose rate in Tokyo is desired by local governmental agencies, autonomous communities and community residents to evaluate the impact of the severe accident at the F1-NPP in detail, to determine ways of safeguarding the health of residents and to assess migration of artificial radionuclides. In this paper, a car-borne survey was carried out for the whole metropolitan Tokyo area in December

2014, and a detailed dose rate distribution map was drawn using the obtained data. Based on the measured data the impact on Tokyo by the F1-NPP accident was estimated. Additionally, mid-and-long term studies are required to investigate migration of artificial radionuclides in large cities such as metropolitan Tokyo. Therefore, as a baseline for future investigation of migration, the detailed radioactive contamination status in Tokyo after the accident was reported.

2. Materials and methods

2.1. Survey route

The ambient dose rate (nGy h^{-1}) from the artificial radionuclides such as ^{134}Cs and ^{137}Cs and the natural radionuclides such as ^{40}K , ^{238}U series and ^{232}Th series were measured on December 6-8, 13, 21, and 27, 2014, in Tokyo, excluding its Pacific island chain that lies in a southeastern direction from the main Japanese island. The weather condition was sunny or cloudy throughout these measurement days, and there was no snow cover or rainfall on them. The survey route encompassed 23 wards (A1 in Fig. 1B), 30 cities, towns and villages (A2 in Fig. 1B). Main roads excluding expressways were used to the extent possible, primarily centered on residential areas (Fig. 2). The survey route was 725 km long. This route map was drawn using the Generic Mapping Tools (GMT) created by Wessel and Smith (1991).

2.2. Car-borne survey

A car-borne survey technique is a common method for fast assessment of dose rate in a large area (Hosoda et al., 2011). The present car-borne survey was carried out using a 3-in \times 3-in NaI(Tl) scintillation spectrometer with a global positioning system (EMF-211, EMF Japan Co., Osaka, Japan). Latitude and longitude at each measurement point were measured at the same time as the count rates in gamma-ray energies of 50 keV – 3.2 MeV were recorded. Measurement of the counts inside the car was performed every 30 s along the route. Car speed was kept around 40 km h^{-1} . The photon peak of ^{40}K ($E_{\gamma} = 1.464 \text{ MeV}$) was used for gamma-ray energy calibration from the channel number and gamma-ray energy before the measurements.

The peak position was determined accurately by smoothing the gamma-ray pulse height distribution. Because the count rate was measured inside the car, shielding by the car body was also corrected by making measurements inside and outside the car at 62 locations (Fig. 2). Those measurements were done above asphalt surfaces because so much of the metropolitan area has been extensively covered with asphalt and concrete, making it impossible to find open fields near roadsides for the measurement. Measurements were recorded over consecutive 30-s intervals during a total recording period of 2 min. A shielding factor was obtained from the slope of the regression line in the relation between count rates inside and outside the car, and count rates inside the car were corrected by multiplying with this shielding factor.

In addition to the above measurements, the gamma-ray pulse height distributions were also measured outside the car for 10 min at 62 locations (Fig. 2). The NaI(Tl) scintillation spectrometer was positioned 1 m above the ground surface. The gamma-ray pulse height distribution measured with the NaI(Tl) scintillation spectrometer was then unfolded using the 22×22 response matrix method (Minato, 2001) and ambient dose rates were calculated. These calculated dose rates were used to estimate the dose conversion factor ($\text{nGy h}^{-1}/\text{cps}$) from the count rates outside the car to the dose rates. Because detection of the photon peak of each gamma ray is impossible in the 30-s measurement in the car-borne survey on roads, ambient dose rates on the roads were estimated by multiplying the dose conversion factor by the corrected inside count rates. In this study, the dose conversion factor was obtained from the slope of the regression line in the relation between corrected inside count rates and ambient dose rates obtained at 62 locations.

All data obtained from the car-borne survey were plotted on the distribution map of the ambient dose rate in Tokyo using GMT (Wessel and Smith, 1991) and compared with data measured in 2003 (Inoue et al., 2015a). A minimum curvature algorithm was used for the data interpolation by GMT. This is the method for interpolating data by presuming a smooth curved surface from the data of individual points. Additionally, the calculated ambient dose rates obtained at 62 locations (Fig. 2) were separated as artificial radionuclides (^{134}Cs and ^{137}Cs) and natural radionuclides (^{40}K , ^{238}U series and ^{232}Th series) using the 22×22 response matrix

method. The obtained gamma-ray pulse height distribution was converted to the energy bin spectrum of incident gamma-rays which is a distribution of gamma-ray flux density to each energy bin. The energy intervals for the bins were given from Minato (2001). The calculation for the 22×22 response matrix for the 3-in \times 3-in NaI(Tl) scintillator was done using the Monte Carlo code, SPHERIX (Matsuda et al., 1982). The gamma-ray flux density and dose rate per unit solid angle are assumed to be almost isotropic in a natural environment. After unfolding the gamma-ray pulse height distribution, clear peaks from ^{134}Cs (bin numbers 6 and 8, energy range: 0.55 – 0.65 MeV and 0.75 – 0.85 MeV), ^{137}Cs (bin number 7, energy range: 0.65 – 0.75 MeV), ^{40}K (bin number 14, energy range: 1.39 – 1.54 MeV), ^{214}Bi (bin numbers 16 and 18, energy range: 1.69 – 1.84 MeV and 2.10 – 2.31 MeV) and ^{208}Tl (bin number 20, energy range: 2.51 – 2.72 MeV) were observed in the spectrum. The contributions from natural and artificial radionuclides could be separated using these techniques. The detailed method has been reported by Minato (2001).

3. Results and discussion

3.1. Shielding and dose conversion factors

A shielding factor is influenced by several factors such as the type of car used in the survey, the number of passengers and the dosimeter position inside the car. A number of previous reports published the shielding factor as 1.4 to 1.9 (Hosoda et al., 2011; Inoue et al., 2015b; Maedera et al., 2015; Inoue et al., 2016). Fig. 3A shows the correlation between count rates inside and outside the car obtained at 62 locations (Fig. 2). The shielding factor and the standard uncertainty (Joint Committee for Guides in Metrology, 2008) were calculated to be 1.33 and 0.07, respectively.

The correlation between dose rate (nGy h^{-1}) calculated from the software using the 22×22 response matrix method (Minato, 2001) and total count rate outside the car is shown in Fig. 3B. The dose rate conversion factor and standard uncertainty were evaluated as 0.15 and 0.01 ($\text{nGy h}^{-1}/\text{cps}$). In the method for determining the ambient dose rate from count rate, the dispersion of dose conversion coefficients are affected by the abundance ratio of ^{40}K , ^{238}U , ^{232}Th

(Shimo et al., 1999), ^{134}Cs and ^{137}Cs . The decision coefficients (R^2) obtained from measurements in 2014 and in 2003 (Inoue et al., 2015a) were 0.759 ($n = 62$) and 0.671 ($n = 27$), respectively.

Compared to those measured in other previous reports in India ($R^2 = 0.964$, $n = 34$) and Brunei (correlation coefficient = 0.97, $n = 16$) (Hosoda et al., 2015; Lai et al., 1996), decision coefficients calculated for metropolitan Tokyo had lower values. In metropolitan Tokyo, stone quarried from adjacent prefectures has been utilized to construct paved roads. Therefore, because the abundance ratio of the natural radionuclides in quarried stone differed depending on the production areas of the stone, mid-level correlations were exhibited by the measurements in metropolitan Tokyo. While the relative standard deviation of the ratios of total count rates to the dose rates at each measurement point was given as 8% in this study, this value was slightly higher compared to previously reported values (3 – 4%) (Inoue et al., 2012; Minato, 2015). However, the dose conversion factor that was determined from measurements on Izu-Oshima Island (Maedera et al., 2015) was almost the same as the present value obtained using the same NaI(Tl) scintillation spectrometer in 2014. Thus, the difference of measurement points for dose conversion factor is likely negligible. Both shielding factor and dose rate conversion factor were used with Eq. (1) to calculate the ambient dose rate (nGy h^{-1}) outside the car 1 m above the ground surface (D_{out}):

$$D_{out} = C_{in} \times 1.33 \times 0.15 \quad (1)$$

where C_{in} is count rate (cps) inside the car obtained by the measurements for 2 min.

3.2. Distribution of ambient dose rate in Tokyo

The average ambient dose rate (range) in the whole area of Tokyo measured in 2014 was 60 nGy h^{-1} (23 – 142 nGy h^{-1}). According to the Tokyo Metropolitan Government (2011), the average ambient dose rate measured at 100 locations in June 2011 was 61 nGy h^{-1} (30 – 200 nGy h^{-1}). Thus, the average dose rate in metropolitan Tokyo has not significantly changed in the past 4 y. Compared with the ambient dose rate before the accident measured in 2003 (i.e., 49

nGy h⁻¹, range of 18 – 76 nGy h⁻¹) (Inoue et al., 2015a), the average ambient dose rate measured in this study was still 24% higher. Additionally, by comparing to the average ambient dose rate for all of Japan (i.e., 50 nGy h⁻¹) (Furukawa and Shingaki, 2012), the average dose rate measured in 2014 was 22% higher.

Fig. 4A shows the distribution map of ambient dose rate in air in Tokyo in 2014. This map was drawn using 4,018 data. Higher ambient dose rates were observed for both eastern and western ends of Tokyo. The average ambient dose rates (ranges) in eastern ($n = 2,010$) and western ($n = 2,255$) areas (i.e., A1 and A2 areas in Fig. 1B) were 60 nGy h⁻¹ (23 – 142 nGy h⁻¹) and 61 nGy h⁻¹ (32 – 102 nGy h⁻¹), respectively. Fig. 4B shows the distribution map of the ambient dose rate measured in 2003 ($n = 669$) (Inoue et al., 2015a). This map and the map for 2014 were both drawn with the same magnification and gradation scale using the GMT. Before the accident, the average ambient dose rates in A1 and A2 areas were 47 nGy h⁻¹ (18 – 61 nGy h⁻¹) and 52 nGy h⁻¹ (34 – 76 nGy h⁻¹), respectively. Compared with those dose rates, the average dose rates after the accident were increased 27% in A1 area and 17% in A2 area.

Table 1 shows ambient dose rates measured in 2014 and 2003 (Inoue et al., 2015a) in all municipalities of Tokyo. In A1 and A2 areas, the highest ambient dose rates (> 70 nGy h⁻¹) were observed in Katsushika Ward (#22 in Fig. 1B), Hinohara Village and Okutama Town (#52 and #53 in Fig.1B) that are located on eastern and western ends of Tokyo. In addition, the higher dose rates (> 60 nGy h⁻¹) areas had expanded towards the southwest from Katsushika Ward and towards the southeast from Okutama Town. According to the air-borne radiation monitoring during August 2011 to May 2012 (Torii et al., 2012; Yuuki et al., 2014), higher dose rates were observed for western areas of Gunma and Saitama Prefectures (Fig. 1A). The high dose rate areas then extended towards the southeast direction (i.e., western Tokyo). In addition, higher dose areas were also observed for the south area of Ibaraki Prefecture and the northeastern area of Chiba Prefecture (Fig. 1A) and then they extended toward the southwest direction (i.e., eastern Tokyo). Thus, these two shifts might have influenced ambient dose rates on the western and eastern ends of Tokyo.

It was difficult to estimate in detail the impact on ambient dose rate from the F1-NPP accident in Tokyo using only data reported after the accident (Yuuki et al., 2014), however, it becomes possible by comparing dose rates measured before the accident. For example, the same higher dose rates ($> 70 \text{ nGy h}^{-1}$) were observed for eastern and western ends, but the increase rate of ambient dose rate was significantly different. The western area of Tokyo including Okutama Town has a naturally higher dose rate (61 nGy h^{-1}) because it is mainly formed by black shale which is a sedimentary rock and 98% of this area is covered with forest (Fig. 1B) (Furukawa and Shingaki, 2012; Inoue et al., 2015a). For a more detailed analysis, Fig. 5 shows ambient dose rates from the artificial radionuclides (^{134}Cs and ^{137}Cs). Those dose rates were calculated using the 22×22 response matrix method (Minato, 2001). The ambient dose rates from artificial radionuclides in A1 ($n = 26$) and A2 ($n = 36$) areas were 8 nGy h^{-1} ($8 - 19 \text{ nGy h}^{-1}$) and 4 nGy h^{-1} ($0 - 12 \text{ nGy h}^{-1}$), respectively. Thus, the impact on ambient dose rate from artificial radionuclides on the eastern side of Tokyo was twice as high as that on the western side.

The standard uncertainties of one time measurement (30 s) can be calculated from the measured value. The obtained range of counts inside the car was 3450 – 21570 (counts per 30 s) in this study. The standard uncertainty depending on measured counts was calculated to be 118 – 294 (counts per 30 s). The range of relative standard uncertainty for 30 s measurements was also given as 1.4% – 3.4%. Here, the relative standard uncertainties for the shielding factor, dose conversion factor, traceability of the dose rate, and the dose calculation procedure by the response matrix method were given as 5.4%, 7.2%, 4.1% ($k = 2$) (Pony Industry Co., Ltd., Osaka, Japan), and 5.0% (EMF Japan Co., Osaka, Japan), respectively. Thus, the maximum combined relative standard uncertainty to the estimated ambient dose rate in this study was calculated to be 11.1%. However, the real combined relative standard uncertainty would be estimated as more than 11.1% because the uncertainty for the repeated measurement results at the same place in repeated paths could not be considered in this study.

The external effective dose rates ($\mu\text{Sv h}^{-1}$) based on data obtained in December 2014 and in September 2003 (Inoue et al., 2015a) were given as $0.45 \mu\text{Sv h}^{-1}$ and $0.36 \mu\text{Sv h}^{-1}$ using

the dose conversion factor from the dose rate to the effective dose for adults ($0.748 \pm 0.007 \text{ Sv Gy}^{-1}$) (Moriuchi et al., 1990). Thus, the effective dose rate has increased 22% compared to that in 2003. In addition, as the effective dose rate in Japan by terrestrial gamma-rays is $0.38 \mu\text{Sv h}^{-1}$ (Abe et al., 1981), the effective dose rate for the whole Tokyo area in December 2014 was 15% higher than the value for all of Japan. Actually, estimated external effective dose rates in December 2014 might be lower compared to the above value ($0.45 \mu\text{Sv h}^{-1}$) because the occupancy factor (0.9 for indoors, 0.1 for outdoors, for residents in metropolitan Tokyo) (Statistics Bureau, Ministry of Internal Affairs and Communications, Japan, 2014) and the ratio of indoor dose rate to outdoor dose rate (i.e., dose reduction factor) will be considered for the estimation. The general dose reduction factor for artificial radionuclides of 0.4 was used for wooden houses by the International Atomic Energy Agency (1979). However, metropolitan Tokyo has many kinds of residential spaces such as 1 or 2 story wooden houses, 1 to 5 story rebar concrete houses, 1 to 60 story high-rise apartments, and basements. Since the dose reduction factor depends heavily on the structures and locations, there is a limitation to estimate the effective dose rate accurately for residents of metropolitan Tokyo. In addition, the dose reduction factor depends on the energy of the gamma-rays. Thus, this factor for both natural and artificial radionuclides has to be considered. Thus, if a uniform dose reduction factor is utilized when the effective dose rate is calculated for the residents of metropolitan Tokyo, the effective dose rate would include large uncertainties.

The dose rates measured above roads are generally lower than those in surrounding fields in contaminated areas because contamination can be washed away more easily by rain (Hosoda et al., 2011). Thus, if obtained dose rates above asphalt surfaces are utilized, the determined effective dose might be underestimated. In the authors' experience (Inoue et al., 2015b) however, dose rates observed above asphalt surfaces were higher than those in surrounding fields in Katushika Ward (Fig 1B, #22). Especially, higher dose rates were observed above highways and main city streets. The asphalt paving materials in recent use for highways and main city streets are porous mixtures. Those roads have higher percentages of voids compared with older local roads. Thus, it was considered that many artificial

radionuclides had accumulated inside the porous asphalt. Metropolitan Tokyo has large areas covered with such asphalt materials, and Tokyo residents are living in such areas. Therefore, the outside effective dose can be properly calculated from dose rates measured on asphalt surfaces.

4. Conclusion

The car-borne survey using a NaI(Tl) scintillation spectrometer was done in Tokyo in 2014 and results were compared to dose rates obtained in 2003. The ambient dose rates (range) in 2014 were found to be 60 nGy h⁻¹ (23 – 142 nGy h⁻¹) for the whole Tokyo area, 60 nGy h⁻¹ (23 – 142 nGy h⁻¹) for the eastern end of Tokyo and 61 nGy h⁻¹ (32 – 102 nGy h⁻¹) for the western end. These values were 24%, 27% and 17% times higher than those of 2003. Similar higher ambient dose rates (> 70 nGy h⁻¹) were observed for the eastern and western ends; furthermore, the contribution ratio from the artificial radionuclides (¹³⁴Cs and ¹³⁷Cs) to the ambient dose rate in the eastern end of Tokyo was twice as high as that of the western end. The estimated effective dose rate based on dose rate measured in December 2014 and September 2003 was 0.45 μSv h⁻¹. This value was 22% higher than the value before the accident.

Acknowledgments

This work was funded by the strategic research fund of Tokyo Metropolitan University.

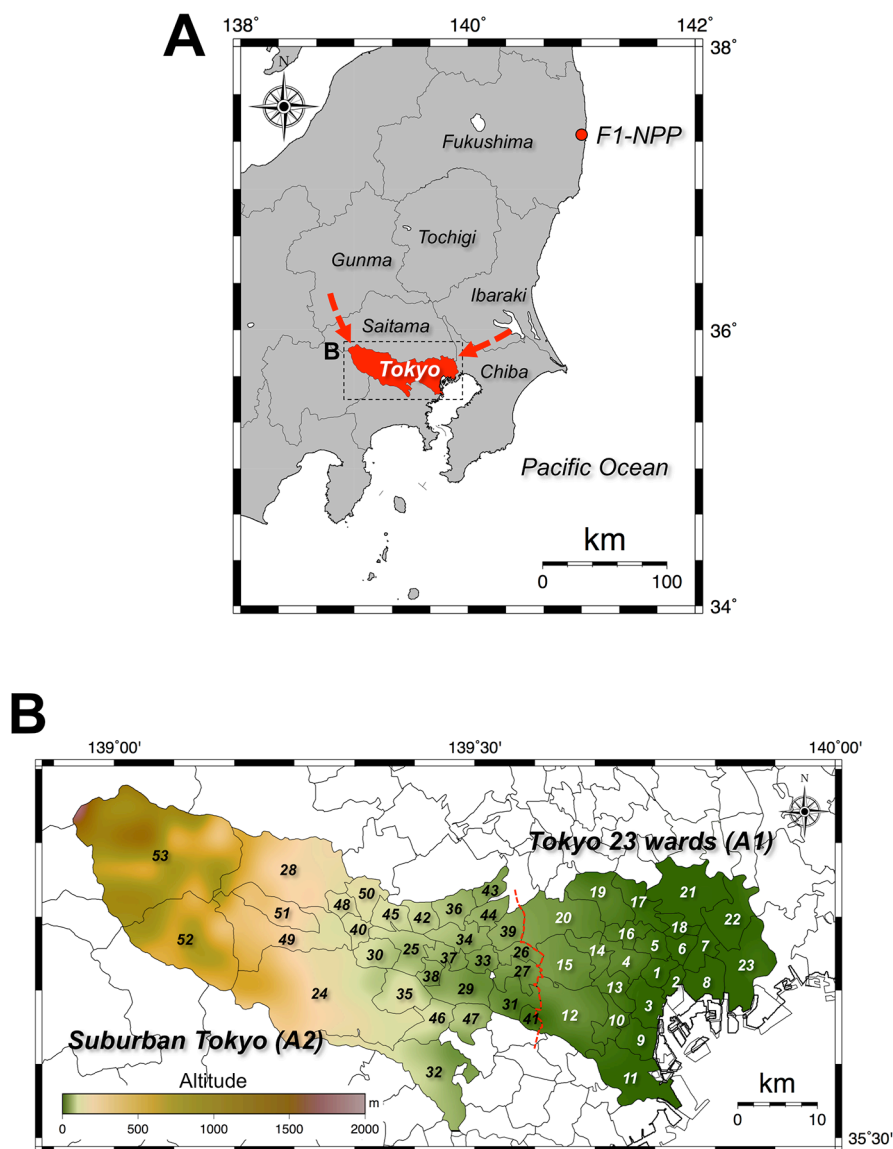


Fig. 1. A Map showing locations of Tokyo and the Fukushima Daiichi Nuclear Power Plant (F1-NPP). Red arrows explain deposition pathways of artificial radionuclides from F1-NPP (Torii et al., 2012; Yuuki et al., 2014). B Map showing Tokyo municipalities consisting of 23 wards and 30 cities, towns and villages. The number for each administrative district (#1 - #53) is an ID number that is given in this paper by reference to the Japanese Industrial Standards. The color scale gives the altitudes within the districts. These maps were drawn using the Generic Mapping Tools of Wessel and Smith (1991).

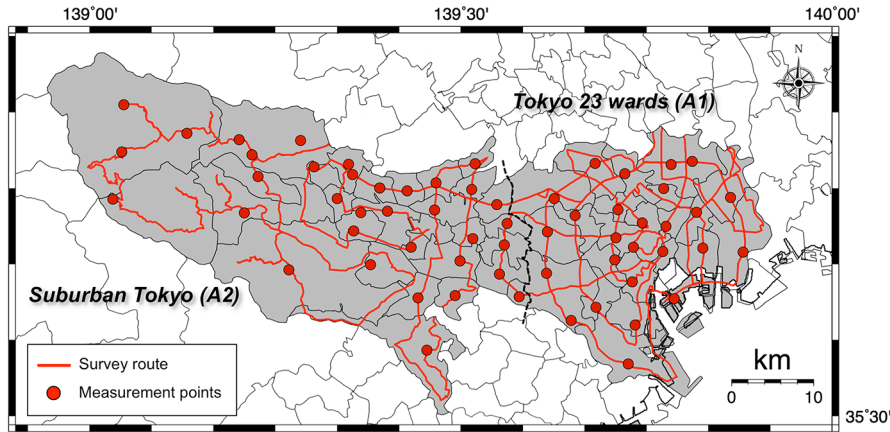


Fig. 2. The survey route for measuring the ambient dose rate in Tokyo. A car-borne survey was carried out using a 3-in \times 3-in NaI(Tl) scintillation spectrometer in December 2014. Total distance traveled was 725 km. The fixed-point measurements outside the car were also performed for 10 min at 62 locations.

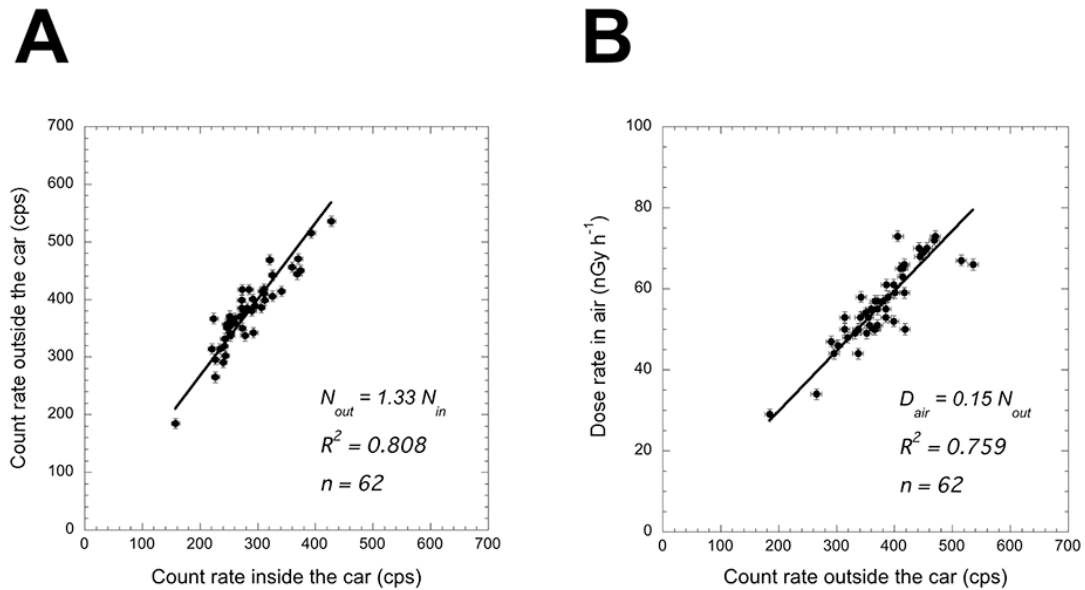


Fig. 3. A Correlation between count rates inside and outside the car. B Correlation between dose rates in air and count rates outside the car. The dose rates were calculated using software that implemented the 22×22 response matrix method (Minato, 2001). The slopes of these regression lines were used as the shielding factor and the dose conversion factor.

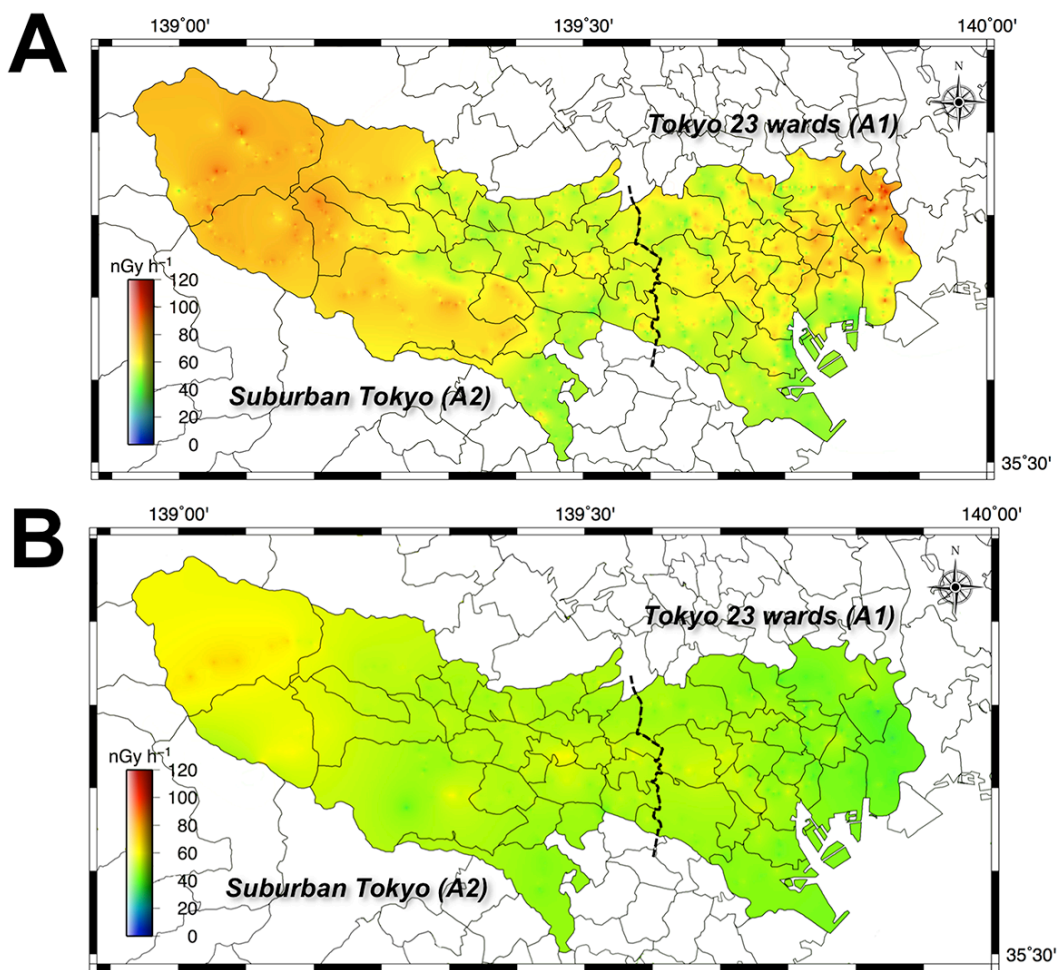


Fig. 4 The distribution maps of ambient dose rate in Tokyo. A Rate measured in 2014. B Rate measured in 2003 (Inoue et al., 2015a). Those maps were drawn using 4,018 data for 2014 and 662 data for 2003.

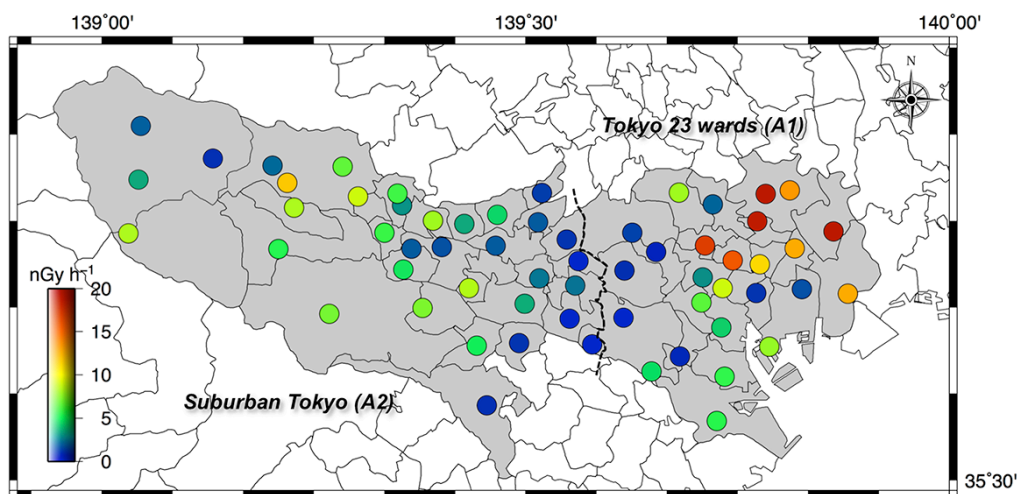


Fig. 5 Ambient dose rates from the artificial radionuclides (^{134}Cs and ^{137}Cs) at 62 locations in Tokyo. The obtained ambient dose rates were separated as artificial radionuclides and natural radionuclides (^{40}K , ^{238}U series and ^{232}Th series) using the response matrix method (Minato, 2001).

References

Abe, S., Fujitaka, K., Abe, M., Fujimoto, K., 1981. Extensive Field Survey of Natural Radiation in Japan. *J. Nucl. Sci. Technol.* 18(1), 21-45.

Andoh, M., Nakahara, Y., Tsuda, S., Yoshida, T., Matsuda, N., Takahashi, F., Mikami, S., Kinouchi, N., Sato, T., Tanigaki, M., Takamiya, K., Sato, N., Okumura, R., Uchihori, Y., Saito, K., 2015. Measurement of air dose rates over a wide area around the Fukushima Dai-ichi Nuclear Power Plant through a series of car-borne surveys. *J. Environ. Radioact.* 139, 266-280.

Furukawa, M., Shingaki, R., 2012. Terrestrial Gamma Radiation Dose Rate in Japan Estimated before the 2011 Great East Japan Earthquake. *Radiat. Emerg. Med.* 1, 11-16.

Hosoda, M., Tokonami, S., Sorimachi, A., Monzen, S., Osanai, M., Yamada, M., Kashiwakura, I., Akiba, S., 2011. The time variation of dose rate artificially increased by the Fukushima nuclear crisis. *Sci. Rep.* 1, 87 (doi:10.1038/srep00087).

Hosoda, M., Tokonami, S., Omori, Y., Sahoo, SK., Akiba, S., Sorimachi, A., Ishikawa, T., Nair, RR., Jayalekshmi, PA., Sebastian, P., Kwaoka, K., Akata, N., Kudo, H., 2015. Estimation of external dose by car-borne survey in Kerala, India. *PLoS One.* 10(4): e0124433 (doi: 10.1371/journal.pone.0124433).

Inoue K, Hosoda M, Sugino M, Simizu H, Akimoto A, Hori K, Ishikawa T, Sahoo SK, Tokonami S, Narita H, Fukushi M., 2012. Environmental radiation in Izu-Ooshima Island After the accident of Fukushima Daiichi Nuclear Power Plant. *Radiat. Prot. Dosim.*, 152, 234-237.

Inoue, K., Hosoda, M., Fukushi, M., Furukawa, M., Tokonami, S., 2015a. Absorbed dose rate in air in metropolitan Tokyo before the Fukushima Daiichi Nuclear Power Plant accident. *Radiat. Prot. Dosim.* 167(1-3), 231-234.

Inoue, K., Hosoda, M., Shiroma, Y., Furukawa, M., Fukushi, M., Iwaoka, K., Tokonami, S., 2015b. Changes of ambient gamma-ray dose rate in Katsushika Ward, metropolitan Tokyo before and after the Fukushima Daiichi Nuclear Power Plant accident. *J. Radioanal. Nucl. Chem.* 303, 2159-2163.

Inoue, K., Tsuruoka, H., Le Van, T., Fukushi, M., 2016. Contribution ratios of natural radionuclides to ambient dose rate in air after the Fukushima Daiichi Nuclear Power Plant accident. *J. Radioanal. Nucl. Chem.* 307, 507-512.

International Atomic Energy Agency, 1979. Planning for off-site response to radiation accidents in nuclear facilities, IAEA-TECDOC-225, Vienna.

Joint Committee for Guides in Metrology, 2008. Evaluation of measurement data -Guide to the expression of uncertainty in measurement, JCGM 100:2008.

http://www.bipm.org/utis/common/documents/jcgm/JCGM_100_2008_E.pdf

(accessed 19.1.2016).

Kinoshita, N., Sueki, K., Sasa, K., Kitagawa, J., Ikarashi, S., Nishimura, T., Wong, Y.S., Satou, Y., Handa, K., Takahashi, T., Sato, M., Yamagata, T., 2011. Assessment of individual radionuclide distributions from the Fukushima nuclear accident covering central-east Japan. *Proc. Natl. Acad. Sci. U.S.A.* 108, 19526-19529.

Koo, Y.-H., Yang, Y.-S., Song, K.-W., 2014. Radioactivity release from the Fukushima accident and its consequences: A review. *Prog. Nucl. Energy* 74, 61-70.

Lai, KK., Hu, SJ., Kodaira, K., Minato, S., 1996. A carborne survey of terrestrial gamma-ray dose rates in Brunei darussalam. *Radioisot.* 45, 696-699 (in Japanese with English abstract).

Maedera, F., Inoue, K., Sugino, M., Sano, R., Furue, M., Shimizu, H., Tsuruoka, H., Le Van, T., Fukushi, M., 2015. Natural Variation of Ambient Dose Rate in the Air of Izu-Oshima Island after the Fukushima Daiichi Nuclear Power Plant Accident. *Radiat. Prot. Dosim.* (doi: 10.1007/s10967-015-4164-8).

Matsuda, H., Furukawa, S., Kaminishi, T., Minato, S., 1982. A new method for evaluating weak leakage gamma-ray dose using a $3''\phi \times 3''$ NaI(Tl) scintillation spectrometer (I) Principle of background estimation method. Report of the Government Industrial Research Institute, 31, 132-146. (in Japanese)

Minato, S., 2001. Diagonal Elements Fitting Technique to Improve Response Matrixes for Environmental Gamma Ray Spectrum Unfolding. *Radioisot.* 50, 463-471.

Minato, S., 2015. A geoscientific background on the distribution of terrestrial gamma ray dose rates in the Japanese Island. *Radioisot.* 66, 535-548 (in Japanese with English abstract).

Ministry of Education, Culture, Sports, Science and Technology - Japan, 2011. Measurements of airborne monitoring for Tokyo and Kanagawa by the Ministry of Education, Culture, Sports, Science and Technology.

http://radioactivity.nsr.go.jp/ja/contents/5000/4897/24/1910_100601.pdf

(in Japanese, accessed 19.10.2015).

Morino, Y., Ohara, T., Nishizawa, M., 2011. Atmospheric behavior, deposition, and budget of radioactive materials from the Fukushima Daiichi nuclear power plant in March 2011. *Geophys. Res. Lett.* 38, L00G11.

Moriuchi, S., Tsutsumi, M., Saito, K., 1990. Examination on conversion factors to estimate effective dose equivalent from absorbed dose in air for natural gamma radiations. *Jpn. J. Health Phys.* 25, 121-128 (in Japanese with English abstract).

Shimo, M., Minato, S., Sugino, M., 1999. A survey of environmental radiation Aichi, Gifu and Mie prefectures. *J. Nucl. Sci. Technol.* 41, 954-964 (in Japanese with English abstract).

Statistics Bureau, Ministry of Internal Affairs and Communications, Japan, 2014. Fundamental aspects of social life in 2013.

<http://www.stat.go.jp/data/shakai/2011/pdf/houdou.pdf>

(in Japanese, accessed 7.1.2016).

Stohl, A., Seibert, P., Wotawa, G., Arnold, D., Burkhart, J.F., Eckhardt, S., Tapia, C., Vargas, A., Yasunari, T.J., 2012. Xenon-133 and caesium-137 releases into the atmosphere from the Fukushima Dai-ichi nuclear power plant: determination of the source term, atmospheric dispersion, and deposition. *Atmos. Chem. Phys.* 12, 2313-2343.

Tokyo Metropolitan Government, 2011. Press Releases. Measurements of radiation dose in air of 100 locations in Tokyo.

<http://www.metro.tokyo.jp/INET/OSHIRASE/2011/06/2016o800.htm>

(in Japanese, accessed 19.10.2015).

Tokyo Metropolitan Institute of Public Health, 2015. Measurement results of environmental radiation levels in Tokyo. <http://monitoring.tokyo-eiken.go.jp/en/index.html> (accessed 19.10.2015).

Torii, T., Sanada, Y., Sugita, T., Kondo, A., Shikaze, Y., Takahashi, M., Ishida, M., Nishizawa, Y., Urabe, Y., 2012. Investigation of Radionuclide Distribution Using Aircraft for Surrounding Environmental Survey from Fukushima Dai-ichi Nuclear Power Plant. JAEA-Technology 036. <http://jolissrch-inter.tokai-sc.jaea.go.jp/pdfdata/JAEA-Technology-2012-036.pdf> (in Japanese with English abstract, 19.10.15.).

Wessel, P., Smith W., 1991. Free software helps map and display data. Eos. Trans. AGU 72, 441-446.

Yoshikawa, N., Obara, H., Ogasa, M., Miyazu, S., Harada, N., Nonaka, M., 2014. ¹³⁷Cs in irrigation water and its effect on paddy fields in Japan after the Fukushima nuclear accident. Sci. Total Environ. 481, 252-259.

Yuuki, Y., Maeshima, M., Hirata, R., Matsui, M., 2014. Airborne radiation monitoring in the Fukushima Daiichi nuclear power plant accident. Oyo Technical Report 33, 105-115. http://www.oyo.co.jp/oyocms_hq/wp-content/uploads/2015/03/04_P-THEM_OYO2A4r2.pdf (in Japanese with English abstract, accessed 19.10.2015).

Zhang, W., Korpach, E., Berg, R., Ungar, K., 2013. Testing of an automatic outdoor gamma ambient dose-rate surveillance system in Tokyo and its calibration using measured deposition after the Fukushima nuclear accident. J. Environ. Radioact. 125, 93-98.